

# Dynamical Quantum Hysteresis

Arnab Das

*Condense Matter and Statistical Physics Division,*

*The Abdus Salam International Center for Theoretical Physics, Strada Costiera 11, 34014 Trieste, Italy*

(Dated: March 22, 2019)

Here we report for the first time, the phenomenon of dynamical quantum hysteresis (DQH) and some drastic non-classical effects associated to it. We demonstrate the phenomenon in one-dimensional Ising model driven by a sinusoidal transverse field (symmetric about zero) at high frequency  $\omega$  at zero temperature. DQH is manifested by the symmetry-breaking characterized by a non-zero value of the long-time average of the transverse magnetization, (the dynamical order parameter) close to its initial value. Interesting non-classical effects, namely, non-monotonic behavior of the order parameter with  $\omega$  (showing curious peak structures), finite response at infinite driving frequency (origin of this is connected to the fact that the high-frequency regime is dominated by the so-called zero-photon process), and stronger localization with increasing driving amplitude are observed. All the features are deduced analytically with exact asymptotic results. The analytical results are in excellent agreement with exact numerical results calculated for a system of  $10^4$  spins. Different experimental set-ups are discussed where the phenomenon may be observed.

Hysteresis is a characteristic non-equilibrium response of a system to a periodic drive with the driving period much shorter than the intrinsic relaxation time of the system. Classically, a macroscopic relaxation time for the system to follow the instantaneous equilibrium state in a driven system often derives its origin from the presence of available metastable states (local energy/free-energy minima) that hold the system back as the field moves on. Hysteresis is hence observed, for example, when a system is driven about a first order phase transition point, [1, 2, 3, 4], or in presence of quenched disorders [5]. As a generic representative of the classical scenario let us consider a classical Ising model below the critical temperature  $T_C$ , in a longitudinal driving field oscillating symmetrically about zero. The drive will periodically elevate and lower the two free-energy minima (corresponding to upward and downward magnetization), one with respect to the other. The quasi-static (hysteresis-free) dynamics would require the system following the global instantaneous free energy minimum through out the evolution. But since there is a free-energy barrier between the two minima, there is a macroscopic relaxation time for the system to relax from the higher minimum to the lower one (favored by the instantaneous  $h_l$ ), and if the period of oscillation is lower than this relaxation time, the system fails to follow the instantaneous field. For moderately high frequencies, there will be a phase-lag between the field and the instantaneous magnetization, giving rise to a symmetric hysteresis loop. But for very high frequencies, the system will be trapped dynamically in one of the minima, resulting in a non-zero value of the long-time average of the magnetization - a phenomenon known as dynamical (classical) hysteresis (DCH) [2].

Here we show for the first time that a similar dynamical localization may be observed in a periodically driven quantum system at zero temperature, due to radically different mechanisms (we call it dynamical quantum hys-

teresis or DQH). Instead of an intrinsic relaxation time set by some available local energy-minima or metastable states, here the inherent timescale that competes with the driving period is set by the slowness of the evolution required for the instantaneous state of the system to follow the ground state of the time-dependent Hamiltonian adiabatically. Strong localization may occurs in the quantum case as a result of loss of adiabaticity, and additionally, due to dynamics-dependent destructive interference effect, even in absence of any local energy minima and energy barriers. The phenomenon is completely different from the quantum effects on hysteresis reported so far [6], where in contrast to our case, quantum resonant tunneling actually helps relaxation.

To demonstrate the phenomenon we consider one dimensional transverse field Ising model (TFIM) [7], which played a bench-marking role in hosting a large number of important studies in non-equilibrium quantum dynamics [8]-[19], mostly concentrating around the effect of linear quench across the critical points/line on the density of defect produced, giving rise to the quantum versions of the Kibble-Zurek effect [20, 21]. The Hamiltonian for the TFIM with a sinusoidal transverse field may be given as follows.

$$H(t) = -\frac{1}{2} \left[ \sum_{i=1}^N \sigma_i^x \sigma_{i+1}^x + h_z(t) \sum_{i=1}^N \sigma_i^z \right]; \quad (1)$$

$$h_z(t) = h_0 \cos(\omega t).$$

Here,  $\sigma_i^{x/z}$  represents the  $x/z$  component of the Pauli spin sitting at the  $i$ -th site, and  $h_z(t)$  denotes the transverse field oscillating in time  $t$  with frequency  $\omega$  and amplitude  $h_0$ . Hamiltonian (1), with periodic boundary condition, when projected to the even-fermionic subspace (where lies the global ground state) via Jordan-Wigner transformation followed by Fourier transform, reduces to

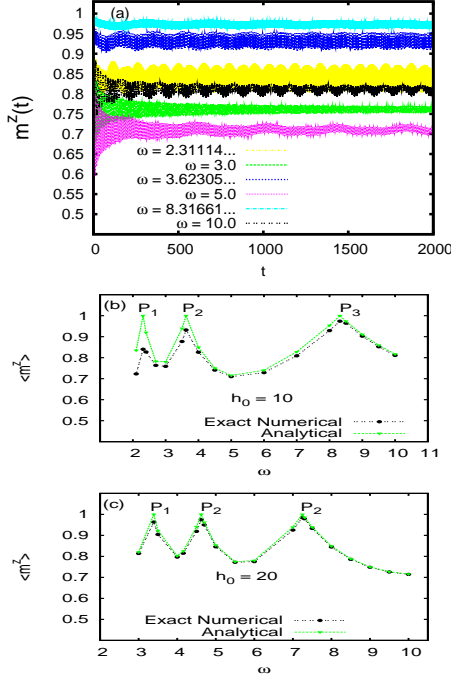


FIG. 1: Top panel (color online) (a) shows the variation of transverse magnetization  $m^z(t)$  with time, for the driving amplitude  $h_0 = 10$  (color online). The frequencies in decreasing order of average  $m^z$  (from top to bottom) are  $\omega = 8.31661\dots$ ,  $\omega = 3.62305\dots$ ,  $\omega = 2.31114\dots$ ,  $\omega = 10.0$ ,  $\omega = 3$  and  $\omega = 5$ . Among them, the first three correspond to the first three zero's of  $J_0(2h_0/\omega)$  at  $2h_0/\omega = 2.4048\dots$ ,  $5.5200\dots$  and  $8.6537\dots$  respectively. The middle panel (b) shows  $\langle m^z \rangle$  which is the long-time steady average of  $m^z$ , as a function of  $\omega$  for  $h_0 = 10$ . Here the peaks  $P_1$ ,  $P_2$  and  $P_3$  corresponds to the frequencies  $\omega = 2.31114\dots$ ,  $\omega = 3.62305\dots$  and  $\omega = 8.31661\dots$  respectively. Analytical results  $\langle m^z \rangle = \frac{1}{1+|J_0(2h_0/\omega)|}$  is compared with exact numerical result for  $10^4$  spins. The lower panel (c) shows the same as in (b), for  $h_0 = 20$ . The peaks  $P_1, P_2$  and  $P_2$  corresponds to  $\omega = 3.392\dots, 4.622\dots$ , and  $7.246\dots$  respectively, which corresponds to the zeros of  $J_0(2h_0/\omega)$  at  $2h_0/\omega = 11.971\dots, 8.653\dots$ , and  $5.520\dots$  respectively.

a direct sum of  $N/2$ -number of  $2 \times 2$  Hamiltonians  $H_k$ 's (see, for example, [11]):

$$H = \bigoplus_{k>0} H_k; \quad H_k = \begin{pmatrix} c_k^\dagger & c_{-k} \\ i\Delta_k & E_k \end{pmatrix} \begin{pmatrix} c_k \\ c_{-k}^\dagger \end{pmatrix} \quad (2)$$

with  $k = \frac{2(n+1)\pi}{N}$ ;  $n = 0, 1, \dots, N/2$  and  $E_k = h_z(t) + \cos k$  and  $\Delta_k = \sin k$ . Here  $c_{\pm k}^\dagger$  and  $c_{\pm k}$  are respectively the creation and the annihilation operators for the Jordan-Wigner fermions ( $k$ -fermions). In this representation, the time-dependent wave function  $|\psi(t)\rangle$  for the system may be expressed as a direct-product of the two-dimensional time-dependent wave functions:  $|\psi(t)\rangle = \bigotimes_{k>0} |\psi_k(t)\rangle$  in  $k$  space, with

$$|\psi_k(t)\rangle = u_k(t)|0_{+k}0_{-k}\rangle + v_k(t)|+k, -k\rangle \quad (3)$$

where  $|0_{+k}0_{-k}\rangle$  and  $|+k, -k\rangle$  represents respectively

the unoccupied and the doubly occupied states of  $\pm k$ -fermion. The time-dependent transverse magnetization in this notation reads

$$m^z(t) = \langle \psi(t) | \sigma^z | \psi(t) \rangle = \frac{4}{N} \sum_{k>0} |v_k(t)|^2 - 1 \quad (4)$$

(dropping the site-index for translational invariance). Now we employ the unitary rotation  $|\psi_k(t)\rangle = \exp\left[\frac{i}{2}(2t \cos k + \frac{2h_0}{\omega} \sin \omega t) \sigma^z\right] |\psi'_k(t)\rangle$  and perform a simple expansion in terms of Bessel's function:  $\exp[iz \sin \theta] = \sum_{n=-\infty}^{+\infty} J_n(z) e^{in\theta}$ ,  $J_n(z)$  being the Bessel's function of the first kind with integer order  $n$  [22]. The rotated wave function

$$|\psi'_k(t)\rangle = u'_k(t)|0_{+k}, 0_{-k}\rangle + v'_k(t)|+k, -k\rangle \quad (5)$$

follows the time-dependent Schrödinger equation

$$i \frac{d}{dt} |\psi'_k(t)\rangle = H'_k(t) |\psi'_k(t)\rangle, \quad (6)$$

with the transformed Hamiltonian  $H'_k(t)$  given by

$$H'_k(t) = -\Delta_k \begin{pmatrix} 0 & i \sum_{n=-\infty}^{\infty} R_n \\ -i \sum_{n=-\infty}^{\infty} R_n^* & 0 \end{pmatrix}; \quad (7)$$

$$R_n = J_n\left(\frac{2h_0}{\omega}\right) e^{-i(n\omega + 2 \cos k)t}. \quad (8)$$

We note that  $|u'_k(t)|^2 = |u_k(t)|^2$  and  $|v'_k(t)|^2 = |v_k(t)|^2$ .

In order to investigate the localization, we start with the ground state of the Hamiltonian  $H(t=0)$  in Eq. (1) with  $h_0 \gg 1$  (highly polarized in  $+z$ -direction). The dynamical localization may now be measured simply by monitoring the long-time average of  $m^z$ :

$$\langle m^z \rangle = \lim_{T_f \rightarrow \infty} \frac{1}{T_f} \int_0^{T_f} m^z(t) dt \quad (9)$$

The resulting time evolution of  $m^z$ , obtained by exact numerical integration (for  $10^4$  spins) of the time-dependent Schrödinger equation for many sweeps as shown in Fig. 1, panel (a). The figure shows that that in each case,  $m^z$  remains confined within a narrow range in the positive sector (starting with  $m^z \approx 1$ ) for all time, though the field  $h_z$  oscillates symmetrically about zero. Moreover, its long-time average  $\langle m^z \rangle$  is not a monotonic function of  $\omega$ , rather, it shows some peaks appearing at certain values of the driving parameters ( $\omega$  and  $h_0$ ) as shown in (Fig. 1, b,c).

This may be explained in terms of the dynamics of the  $k$ -modes. Eq. of the form (6) can be solved analytically under resonance approximation (RA), which amounts to ignoring all the terms in the off-diagonal sum in  $H'_k(t)$  except for the resonant term  $n = n_r$ , for which the effective frequency  $\Omega_k = |n\omega + 2 \cos k|$  is the smallest. All other faster oscillating terms are neglected. With the initial

condition mentioned above ( $|v_k(0)|^2 \approx 1$ ), the solution of Eq. (6) for any  $n = n_r$  under the RA gives [23]:

$$|v_k(t)|^2 = 1 - \frac{4A_k^2}{4A_k^2 + (2\cos k + n_r\omega)^2} \sin^2(\nu_k t), \quad (10)$$

where  $A_k = \frac{J_{n_r}(2h_0/\omega)\Delta_k}{\frac{1}{2}\sqrt{4A_k^2 + (2\cos k + n_r\omega)^2}}$ . In the concerned high frequency limit ( $\omega \gg 2|\cos k|$ ), we have  $n_r = 0$ . From Eq. (10) one sees (putting  $n_r = 0$ ) that the critical modes ( $k \sim 0, \pi$ ), for which  $\Delta_k = \sin(k) \sim 0$ ,  $|v_k(t)|^2$  oscillates with a vanishing amplitude proportional to  $\Delta_k^2$  and thus contribute to the freezing of  $m^z$  around its initial value. However, for high  $\omega$ , the contribution from the off-critical modes ( $\Delta_k \gg 0$ ) is nontrivial, and results in interesting counter-classical behaviors as follows. For these modes,  $|v_k(t)|^2$  oscillates with an amplitude  $A_k^2/(A_k^2 + \cos^2(k))$  about an average value  $1 - A_k^2/2(A_k^2 + \cos^2(k))$ . For  $J_0(2h_0/\omega) \gg 1$ , these modes follow the field almost adiabatically, but becomes more non-adiabatic as the factor  $J_0(2h_0/\omega)$  becomes smaller. Taking the continuum limit of Eq. (4) and integrating over  $k$ , one obtains a simple formula for  $\langle m^z \rangle$ :

$$\langle m^z \rangle = \frac{2}{\pi} \int_0^\pi dk \left[ \frac{1}{2\pi/\nu_k} \int_0^{2\pi/\nu_k} dt |v_k(t)|^2 \right] - 1 \quad (11)$$

$$= \frac{1}{1 + |J_0(2h_0/\omega)|}. \quad (12)$$

This matches surprisingly well with the peaked-structured profile of  $\langle m^z \rangle$  obtained by exact numerical integration, as shown in Fig. 1 (b) and (c). Here the time-average in the  $T_f \rightarrow \infty$  limit is obtained analytically by simply adding the time-average over a complete cycle for each mode, since  $\nu_k$  is finite for all  $k$ . The peaks occur for certain combinations of  $\omega$  and  $h_0$ , for which  $J_0\left(\frac{2h_0}{\omega}\right) = 0$ . Under this condition, the entire spectrum freezes, resulting in an absolute localization of the system around its initial state for all time. The condition for the dynamical freezing of a two-level system is well-known in the literature as the coherent destruction of tunneling or CDT [24]. Such dynamics-dependent localizations may be interpreted as destructive interference of paths due to periodic driving, as discussed in [25].

The observed non-monotonicity in  $\langle m^z \rangle$  with respect to  $\omega$  is counter-intuitive to the classical notion, since in high-frequency regime, increase in frequency always means more freezing, and hence stronger localization, as observed in DCH [2]. In the limit  $\omega \rightarrow \infty$ ,  $\langle m^z \rangle \rightarrow \frac{1}{2}$ . This result is again quite counter-intuitive; in the  $\omega \rightarrow \infty$  limit, the system is expected to fail to respond at all, and hence would freeze completely to the initial state, and one should have  $\langle m^z \rangle \rightarrow 1$ , be it an elementary mechanical systems like driven harmonic oscillator or be it classical spin systems at finite temperature [2]. The

counter-classical behavior stems from the fact that the high  $\omega$  regime, the dominant process is the resonant process is the zero-photon process ( $n_r = 0$ ) [26]. For any  $n_r \neq 0$ , one would have  $\omega$  in the denominator, and hence  $|v_k|^2 \rightarrow 1 \Rightarrow \langle m^z \rangle \rightarrow 1$ , as  $\omega \rightarrow \infty$  (see Eq. 10), and the classical behavior would have been retrieved.

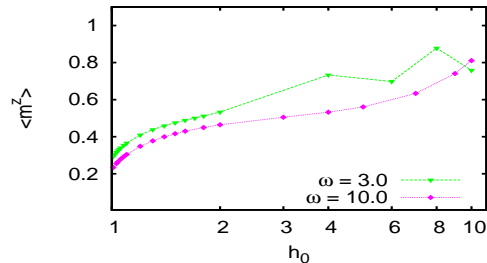


FIG. 2: The plot shows variation of  $\langle m^z \rangle$  (numerical) with  $h_0$  for different  $\omega$ . The counter-classical trend of higher degree of dynamical localization at higher driving amplitude is clear in the monotonically increasing nature of  $\langle m^z \rangle$  with  $h_0$ .

There is another interesting feature of DQH, which is also in contrary with the classical picture. In DCH, as one increases the strength of the driving field, it tends to enforce the system to follow it more closely, and for a strong enough driving field dynamical hysteresis cease to exit [4]. For example, a very strong longitudinal driving field in a classical Ising magnet would effectively flatten the free-energy barrier(s) between the metastable states created as a result of cooperative interaction, and would force the system to follow the field even without much phase lag [27]. In the DCH studies, the localized phase is always observed below a certain value  $h_0(\omega, T)$  of the amplitude of the driving field. As the amplitude is increased beyond that, the dynamical hysteresis is destroyed and the symmetric phase appears. [2]. But in DQH, just the reverse trend is observed, as shown in Fig. 2. The figure shows that a higher freezing (characterized by higher values of  $\langle m^z \rangle$ ) is obtained as  $h_0$  is increased. In the high frequency limit, one can make the approximation  $J_0(x) \approx \sqrt{\frac{2}{\pi x}} \cos(x - \pi/4)$  for  $x \gg \frac{1}{4}$  and the expression (12) reduces to

$$\langle m^z \rangle \approx \langle m^z \rangle_\infty - \frac{\sqrt{\omega} \cos\left(\frac{2h_0}{\omega} - \frac{\pi}{4}\right)}{\sqrt{\pi h_0} + \sqrt{\omega} \cos\left(\frac{2h_0}{\omega} - \frac{\pi}{4}\right)}, \quad (13)$$

where  $\langle m^z \rangle_\infty = \lim_{h_0 \rightarrow \infty} \langle m^z \rangle = 1$ , giving an absolute localization in this limit. Eq. (13) shows  $\langle m^z \rangle_\infty - \langle m^z \rangle$  vanishes as  $h_0^{-\frac{1}{2}}$  with a sinusoidal modulation as  $h_0 \rightarrow \infty$  for a given  $\omega$ . The classically intuitive picture of a stronger drive compelling the system more strongly to follow it, does not hold any more.

Experimental verification of the DQH phenomenon can be achieved in several ways. First, realization of tunable

transverse Ising model using trapped ions [28] opens up a way of verifying our results directly. Similar realization is possible within the broad framework for realizing lattice-spin models with polar molecules in optical lattice [29]. In these systems, the exchange interaction  $J$  have experimental upper-limits (respectively of the order of 22.1 kHz and between 10 – 100 kHz for the cases mentioned above) but can be made arbitrarily small. Hence the range of high  $\omega$  referred here (expressed in the units of  $J$ ) may be brought down to any comfortable range, say of the order of few kHz in both the realizations. The phenomenon of DQH described here can be translated in two and three-dimensional Kitaev model [30, 31], the experimental realization of the former one being proposed already [32]. The study of such hysteresis in random systems in the context of quantum annealing [33, 34, 35] with cyclic schedules would be interesting. The effect of DQH in quantum engineering, particularly, in ac-driven quantum systems [36] might be enormous.

To summarize, we report the phenomenon of dynamical hysteresis in quantum system for the first time. The phenomenon exhibit drastic counter classical features, namely, non-monotonic frequency dependence, finite response at infinite driving frequency (partly attributed to the domination of the zero-photon process) and completely reverse trend in amplitude dependence as observed and expected in the classical cases. We demonstrate the basic features studying one-dimensional Ising model with oscillating transverse field. The demonstration was entirely analytic and is in excellent agreement with the exact numerical calculations.

**Acknowledgments:** The author thanks Bikas K. Chakrabarti, Giuseppe Santoro, Erio Tosatti, Krishnendu Sengupta and Alessandro Silva for useful discussions.

- 
- [1] M. Acharyya and B. K. Chakrabarti Phys. Rev. B **52**, 6550 (1995); M. Acharyya, J. K. Bhattacharjee and B. K. Chakrabarti, Phys. Rev. E **55**, 2392 (1997).
- [2] B. K. Chakrabarti and M. Acharyya, Rev. Mod. Phys. **71**, 847 (1999).
- [3] M. Rao, H. R. K. Krishnamurthy, and R. Pandit, Phys. Rev. B **42**, 856 (1990).
- [4] T. Tomé and M. J. de Oliveira, Phys. Rev. A **41**, 4251 (1990).
- [5] J.P. Sethna, K. Dahmen, S. Kartha, J. A. Krumhansl, B. W. Roberts and J. D. Shore, Phys. Rev. Lett. **70**, 3347 (1993).
- [6] J. R. Friedman, M. P. Sarachik, J. Tejada, and R. Ziolo, Phys. Rev. Lett. **76**, 3830 (1996); E. M. Chudnovsky, Science, **274**, 938 (1996); T. Thorwart, P. Reimann, P. Jung, and R. F. Fox, Chem. Phys. **235** 61 (1998); C. K. Mondal, and S. P. Bhattacharyya, Int. J. Chem. Phys. **83** 11 (2001).
- [7] B. K. Chakrabarti, A. Dutta, and P. Sen, *Quantum Ising Phases and Transitions in Transverse Ising Models*, **m41** Springer-Verlag, Berlin, (1996); S. Sachdev, *Quantum Phase Transition*, Cambridge University Press, Cambridge, (1999).
- [8] B. Damski, Phys. Rev. Lett. **95**, 035701 (2005).
- [9] W. H. Zurek, U. Dorner, and P. Zoller, Phys. Rev. Lett. **95**, 105701 (2005).
- [10] J. Dziarmaga, Phys. Rev. Lett. **95**, 245701 (2005).
- [11] R. W. Cherng, and L. S. Levitov, Phys. Rev. A **73**, 043614 (2006).
- [12] A. Das, K. Sengupta, D. Sen and B. K. Chakrabarti, Phys. Rev. B **74**, 144423 (2006).
- [13] A. Polkovnikov, Phys. Rev. B **72**, 161201(R) (2005); A. Polkovnikov and V. Gritsev, Nature Physics **4**, 477 (2008).
- [14] V. Mukherjee, A. Dutta, and D. Sen, Phys. Rev. B **77**, 214427 (2008); V. Mukherjee and A. Dutta, arXiv:0901.1933 (2008).
- [15] T. Caneva, R. Fazio and G. E. Santoro, Phys. Rev. B **76**, 144427 (2007).
- [16] S. Deng, G. Ortiz, and L. Viola, Euro. Phys. Letts. **84** 67008 (2008).
- [17] K. Sengupta, D. Sen, and S. Mondal, Phys. Rev. Lett. **100** 077204 (2008); D. Sen, K. Sengupta and S. Mondal, Phys. Rev. Lett. **101**, 016806 (2008).
- [18] D. Patané, A. Silva, L. Amico, R. Fazio, and G. E. Santoro, Phys. Rev. Lett. **101**, 175701 (2008).
- [19] S. Miyashita, H. De Raedt and B. Barbara, Phys. Rev. B **79**, 104422 (2009).
- [20] T. W. B. Kibble, J. Phys. A **9**, 1387 (1976).
- [21] W. H. Zurek, Nature **317**, 505 (1985).
- [22] S. Ashhab, J. R. Johansson, A. M. Zagoskin, and F. Nori, Phys. Rev. A **75**, 063414 (2007).
- [23] M. Silverman., *Quantum superposition: counterintuitive consequences of coherence, entanglement, and interference*, Springer, (2008).
- [24] F. Grossmann, T. Dittrich, P. Jung, and P. Hänggi, Phys. Rev. Lett. **67** 516 (1991); M. Grifoni and P. Hänggi, Phys. Rep. **304**, 229, (1998).
- [25] Y. Kayanuma and K. Saito, Phys. Rev. A **77**, 010101(R) (2008).
- [26] L. Ko, M. W. Noel, J. Lambert and T. F. Gallagher, J. Phys. B **32**, 3469 (1999).
- [27] S. Ghosh, R. Parthasarathy, T. F. Rosenbaum and G. Aeppli, Science **296**, 2195 (2002).
- [28] A. Friedenauer, H. Schmitz, J. T. Glueckert, D. Porras and T. Schaetz, Nature Physics **4**, 757 (2008).
- [29] A. Micheli, G. K. Brennen and P. Zoller, Nature Physics **2**, 341 (2006).
- [30] A. Kitaev, Ann. Phys. **321**, 2 (2006).
- [31] S. Mandal and N. Surendran, Phys. Rev. B **79**, 024426 (2009).
- [32] L.-M. Duan, E. Demler and M. D. Lukin, Phys. Rev. Lett. **91**, 090402 (2003).
- [33] T. Kadowaki and H. Nishimori, Phys. Rev. E **58** 5355, (1998).
- [34] A. Das and B. K. Chakrabarti, Rev. Mod. Phys. **80**, 1061 (2008); Santoro G. E. and Tosatti E. (2006), J. Phys. A **39** R393
- [35] J. Brooke, D. Bitko, T. F. Rosenbaum and G. Aeppli, Science **284**, 779 (1999).
- [36] A. V. Ponomarev, S. Denisov and P. Hänggi, Phys. Rev. Lett. **102**, 230601 (2009).